



Received on 24 July 2025; received in revised form, 24 November 2025; accepted, 13 December 2025; published 01 January 2026

IN-SILICO EXPLORATION OF CHYAWANPRASH PHYTOCONSTITUENTS BINDING AFFINITY WITH KEY TARGETS OF HUMAN METAPNEUMOVIRUS

V. H. Bhargavi, Azra Esha, Manali N. Javeri, Mallikarjun and Erumalla Venkatanagaraju *

Department of Life Sciences, Indian Academy Degree College (Autonomous), Hennur Cross, Bangalore - 560043, Karnataka, India.

Keywords:

Dabur Chyawanprash,
Phytochemicals, Human
metapneumovirus (HMPV), *In-silico*
drug discovery, Plant based
therapeutics

Correspondence to Author:

Erumalla Venkatanagaraju

Associate Professor,
Department of Life Sciences,
Indian Academy Degree College
(Autonomous), Hennur Cross,
Bangalore - 560043, Karnataka, India.

E-mail: venkatanagarajue@gmail.com

ABSTRACT: Background: Human Metapneumovirus (HMPV) remains a significant respiratory pathogen without specific antiviral therapy. Traditional Ayurvedic formulations like Dabur Chyawanprash, composed of numerous medicinal plants, may harbor bioactive compounds with antiviral potential. This study explores phytochemicals from Chyawanprash alongside FDA approved drugs; Ribavirin, Penicillin V and Ibuprofen for their suitability as antiHMPV agents using *in-silico* approaches. **Materials and Methods:** A total of 41 medicinal plants were screened, and their phytochemicals evaluated using SwissADME for pharmacokinetic profiling and ProTox-II for toxicity prediction. Compounds with favorable ADMET properties were docked against five essential HMPV targets: polymerase phosphoprotein complex (6U5O), prefusion closed trimer (8W3Q), M2-1 tetramer (4CSA), prefusion trimer (8VT3), and N-P complex (5FVD). Docking was performed using AutoDock Vina interphase of PyRx, and molecular interactions were analyzed *via* Discovery Studio. **Results:** Seven phytochemicals met ADMET and drug likeness criteria, with propanoic acid and 1-butanol demonstrating optimal GI absorption, BBB permeability, and non-toxic profiles. Among targets, Penicillin V and Ribavirin exhibited the strongest binding, particularly with the N-P complex (-7.7 and -7.2 kcal/mol). Isovaleric acid showed high affinity for the polymerase phosphoprotein and M2-1 tetramer, while butyric acid and isoamyl alcohol also demonstrated strong interactions with various viral proteins. **Conclusion:** This *in-silico* study highlights propanoic acid, isovaleric acid, and 1-butanol as promising antiHMPV candidates. The integration of ADMET filtering with molecular docking provides a rational strategy for lead identification from traditional formulations. These findings merit further *in-vitro* and *in-vivo* investigation to validate their therapeutic potential.

INTRODUCTION: Human metapneumovirus (HMPV) is an enveloped, negative sense, single stranded RNA virus belonging to the *Paramyxoviridae* family and *Pneumovirinae* subfamily ¹.

Since its discovery in 2001, HMPV has been recognized as a major etiological agent of acute respiratory infections (ARIs), particularly affecting infants, young children, the elderly, and immunocompromised populations ². It accounts for a substantial portion of lower respiratory tract infections globally and is responsible for significant morbidity and healthcare burden. Despite its clinical significance and seasonal recurrence, no specific antiviral agents or licensed vaccines have yet been approved for HMPV, making therapeutic intervention an unmet need in the domain of

QUICK RESPONSE CODE 	DOI: 10.13040/IJPSR.0975-8232.17(1).315-32 This article can be accessed online on www.ijpsr.com
DOI link: https://doi.org/10.13040/IJPSR.0975-8232.17(1).315-32	

respiratory virology. Structurally and genomically, HMPV shares many similarities with respiratory syncytial virus (RSV), another clinically important paramyxovirus³. However, HMPV exhibits unique immunopathological features, such as differential cytokine responses and evasion of innate immune recognition, which contribute to its persistence and pathogenicity. The HMPV genome encodes for several structural and nonstructural proteins essential for replication, transcription, and host cell entry. Among these, five protein complexes have been structurally resolved and functionally validated as key targets for therapeutic development. These include the nucleoprotein phosphoprotein (N-P) complex, which facilitates genome encapsidation and polymerase cofactor recruitment; the polymerase phosphoprotein complex, which anchors the viral polymerase to the nucleocapsid; the M2-1 tetramer, a transcriptional antiterminator that enhances RNA polymerase processivity; and two prefusion conformations of the viral fusion (F) protein namely, the closed trimer and the prefusion trimer that mediate host cell membrane fusion and viral entry⁴. These proteins are indispensable for maintaining HMPV replication efficiency and virulence, rendering them attractive molecular targets for antiviral design.

Traditional drug discovery approaches based on high throughput screening and empirical validation, although effective, are time-consuming and resource intensive. In recent years, computer aided drug design (CADD) has emerged as a valuable alternative for early stage antiviral drug discovery. *In-silico* screening platforms integrate molecular docking, pharmacokinetic modeling, and toxicity prediction to enable rapid prioritization of bioactive candidates⁵. Molecular docking, in particular, allows for the prediction of ligand receptor binding affinities and interaction patterns within target binding pockets. When coupled with ADMET profiling tools such as SwissADME and ProTox-II researchers can identify lead compounds with optimal physicochemical, pharmacokinetic, and safety characteristics prior to *in-vitro* or *in-vivo* testing. Parallel to synthetic libraries, natural product scaffolds have gained renewed attention as a promising reservoir of bioactive molecules⁶. Among these, phytochemicals derived from traditional systems of medicine such as Ayurveda are being increasingly explored for their therapeutic

potential against infectious diseases. Chyawanprash, a classical polyherbal formulation documented in Ayurvedic pharmacopeias, is traditionally used to boost immunity and respiratory health. Commercial variants such as Dabur Chyawanprash are formulated using a proprietary blend of over 41 medicinal herbs and plant derived substances, many of which have reported antioxidant, immunomodulatory, antimicrobial, and adaptogenic properties⁷. Despite the widespread use of Chyawanprash as a nutraceutical and functional food, its molecular basis of action, particularly in the context of viral inhibition, remains poorly defined. To address this gap, the present study employs a comprehensive *in-silico* framework to assess the therapeutic potential of phytochemicals derived from the medicinal plant components of Dabur Chyawanprash. A total of 655 bioactive compounds were identified from existing phytochemical databases and literature sources. Three FDA approved reference drugs used in HMPV therapy; ribavirin, penicillin and ibuprofen were included in the study to serve as benchmarks for comparative analysis.

This study not only highlights the potential of Ayurvedic phytochemicals as lead antiviral candidates but also demonstrates the value of integrative *in-silico* methods in rapidly assessing large libraries of natural products against structurally defined viral targets. By benchmarking against FDA approved drugs and focusing on molecular level interactions, this investigation contributes to the rational identification of plant derived inhibitors for HMPV and paves the way for further experimental validation and therapeutic development.

MATERIALS AND METHODS:

Selection and Retrieval of Reference Compounds and Phytochemicals: In this study, three reference drugs; ribavirin (37542), penicillin (5904) and ibuprofen (3672) were selected for comparative analysis. A comprehensive list of phytochemicals was compiled from medicinal plants that constitute the Ayurvedic formulation Dabur Chyawanprash. The selected plant species include: *Stereospermum suaveolens*, *Clerodendrum phlomidis*, *Gmelina arborea*, *Aegle marmelos*, *Oroxylum indicum*, *Tribulus terrestris*, *Desmodium gangeticum*, *Uraria picta*, *Solanum indicum*,

Solanum surattense, *Piper longum*, *Pistacia integerrima*, *Vitis vinifera*, *Tinospora cordifolia*, *Terminalia chebula*, *Sida cordifolia*, *Phyllanthus niruri*, *Adhatodavasica*, *Leptadenia reticulata*, *Hedychium spicatum*, *Cyperus rotundus*, *Inula racemosa*, *Martynia annua*, *Phaseolus trilobus*, *Teramnus labialis*, *Pueraria tuberosa*, *Boerhavia diffusa*, *Nymphaea stellata*, *Elettaria cardamomum*, *Cinnamomum zeylanicum*, *Santalum album*, *Dioscorea bulbifera*, *Asparagus racemosus*, *Withania somnifera*, *Embllica officinalis*, *Bambusa bambos*, *Cinnamomum tamala*, *Mesua ferrea*, *Anacyclus pyrethrum*, *Syzygium aromaticum*, and *Crocus sativus*.

Phytochemical constituents corresponding to these medicinal plants were retrieved from the Indian Medicinal Plants, Phytochemistry and Therapeutics (IMPPAT) database⁸. A focused subset of bioactive compounds was selected for further analysis based on their molecular weight and availability of structural information. The selected compounds and their PubChem CIDs are: 1-penten-3-ol (12020); pentadecanoic acid (13849); nonanal (31289); 2-penten-1-ol (5364920); hydroquinone (785); 2-hexenal (5281168); cis-3-hexen-1-ol (5281167); 2-hexen-1-ol (5318042); linalool (6549); 2,4-pentadienal (5986428); pyrrolidine (31268); sterol (1107); gallic acid (370); syringic acid (10742); shikimic acid (8742); vanillic acid (8468); anthraquinone (6780); ethyl gallate (13250); ferulic acid (445858); 4-hydroxycinnamic acid (637542); pyrogallol (1057); flavylum (145858); ascorbic acid (54670067); ephedrine (9294); phenethylamine (1001); hypaphorine (442106); betaine (247); choline (305); vasicine (667496); pseudoephedrine (7028); tridecanoic acid (12530); verbenone (29025); vasicinol (442934); undecanal (8186); deoxyvasicinone (68261); 1-tetradecanol (8209); 1-octene (8125); quinazoline (9210); 1-pentadecanol (12397); dodecane (8182); 4-hydroxybenzoic acid (135); tetradecane (12389); beta-eudesmol (91457); 2,6,6-trimethyl-2-cyclohexen-1-yl (5372174); d-galactose (6036); lauric acid (3893); beta-pinene (14896); myrtenol (10582); beta-bisabolene (10104370); 2-tridecanone (11622); pinocarvone (121719); myrcene (31253); cubebol (11276107); gamma-terpinene (7461); benzyl cinnamate (5273469); p-cymene (7463); hedycaryol (6432240); methyleugenol (7127); cadinene (9548708);

spathulenol (92231); epi-cubebol (91753433); oplopanone (10466745); 2-nonanone (13187); beta-elemene (6918391); alpha-himachalene (520909); 2-dodecanone (22556); 8(12)-drimene (12184338); 3-carene (26049); 4-carvomenthenol (11230); 2-undecanone (8163); 2-methyl-5-propan-2-ylbicyclohex-2-ene (637518); germacrene-1(10); 5-dien-4-ol (5352847); alpha-terpinene (7462); cis-beta-farnesene (5317319); alpha-muurole ne (12306047); (+)-alpha-cadinene (12306048); alpha-eudesmol (92762); proximadio l(165258); humulene epoxide (10704181); humulene (5281520); gamma-muurolene (12313020); gamma-cadinene (6432404); elemol (92138); gammaeudesmol (6432005); agarospirol (21675005); hinesol (10878761); delta-cadinene (441005); ethyl cinnamate (637758); trans-carveol (94221); camphor (2537); alphapinene (6654); carvone (7439); sabinene (18818); alpha-curcumene (92139); trans-sabinol (6429076); selin-11-en-4-alpha-ol (15560330); caryophyllene oxide (1742210); trimethyl-8-methylidenebicyclo undecene (6429301); transcalamenene (6429022); alphacalacorene (12302243); fenchone (1201521); epcubebol (91748749); globulol (12304985); beta-selinene (442393); alpha-phellandrene (7460); beta-caryophyllene (5281515); beta-himachalene (11586487); cis-alpha-bergamotene (6429303); sabinene (10887971); cedrelanol (160799); 6-epi-beta-bisabolol (12300148); eremoligenol (21591456); trans-linalool oxide (6432254); methylisoeugenol (637776); alpha-copaene (19725); muurolol (3084331); tetradecanone (75364); albicanol (171360); dehydro-aromadendrene (526687); furfuryl hexanoate (557222); allo-aromadendrene (42608158); trans-sabinene hydrate (6326181); umbellulol (561871); trans-alpha-bergamotene (6429302); limonene (22311); tricyclododecantrimethyl (11746218); ethyl p-methoxycinnamate (5281783); linalyl acetate (8294); pentamethyldecahydronaphthalene (9548719); benzyl acetate (8785); pentadecane (12391); bicyclohomofarnesal (10037034); terpinolene (11463); epi-gammaeudesmol (6430754); betaphellandrene (442484); norbornyl acetate (101199); alloalantolactone (474518); isotelekin (12304585); dimethyl methylidene hexahydrocyclodecaphuran-2-one (101289712); isoalloalantolactone (182421); 1, 8, 11, 14-heptadecatetraene (5319559); heptadeca-1, 8, 11-

triene (5352709); helenalin (23205); alpha-lonone (5363685); alantolactone (72724); 2-phenylethanol (6054); beta-lonone (5282108); phenylacetonitrile (8794); furfural (7362); dihydroisoalantolactone (6451323); dihydroalantolactone (10633476); telekin (12443309); benzaldehyde (240); alpha-pinene-oxide (439800); isoalantolactone (73285); alpha-farnesene (5281516); pyrazoline (4021); germacranolide (91694425); 2,5-dihydroxybenzoic acid (3469); 2-hydroxycinnamic acid (637540); sinapic acid (637775); 3,4-dihydroxybenzoic acid (72); fraxidin (3083616); levodopa (6047); gluconic acid (10690); pterocarpan (6451349); cyperol (14076601); isocyperol (14076604); cyperene (12308843); d-borneol (6552009); alpha-cyperone (6452086); dimethylocta-2,4,6-trienal (102316377); caryophyllan-2, 6-beta-oxide (6428086); isorotundene (91753591); gamma-gurjunene (90805); beta-thujene (520384); beta-gurjunene (6450812); 8-isopropyl dimethyl-tetrahydronaphthalene (518975); isopropyl-1-methyl - 5 - methylenecyclodeca - 1, 6-diene (91723653); cyperotundone (12308615); humulene epoxyde (5463721); anethole (637563); alphacadinol (10398656); aristolone (165536); bulnesene (16679399); bicycloundecanodimethyl-2,6-bis (methylene)- (527418); isolongifolen-5-one (600416); viridiflorol (11996452); 2-(4-methylphenyl) propan-2-ol (14529); eudesm-7(11)-en-4-ol (6432454); valeranone (171455); betabourbonene (62566); guaial (227829); longifolene (289151); 1-octen-3-ol (18827); (z)-hex-2-enyl acetate (5363374); valeranal (6440942); hexanal (6184); 1-hexanol (8103); hexanoic acid (8892); widdrol (94334); 1-octanol (957); nootkatone (1268142); alpha-cedrene epoxide (122510); alphacampholenal (1252759); tetramethyl-12-oxabicyclododeca-4,7-diene (22559443); isopinocampone (84532); delta-cadinol (3084311); gamma-elemene (6432312); zizanene (12306046); (e)-beta-ocimene (5281553); cedrol (65575); nerolidol (5320128); (s)-cis-verbenol (87839); 3-pinanone (11038); trans-verbenol (89664); 2-[(2r,8r,8as)-8,8a-dimethyl-1,2,3,4,6,7,8,8a-octahydronaphthalen-2-yl] propan-2-ol (9859337); isomustakone (91748747); dillapiole (10231); isokobusone (3860435); beta-rotunol (5321005); patchoulone (5320424); kobusone (6710676); glycerol (1030); methylbenzene (62385); methyl-4-methylidene-6-

propan-2-yl-1b, 2, 3, 5, 5a, 6a-hexahydro-1h-cyclopropa[a] inden-6-ol (6431225); 1-isopropyl-4-methylenebicyclo [3.1.0] hex-2-ene (524198); cyclosativene (519960); p-mentha-1,5-dien-8-ol (519323); limonene oxide, cis (6452061); cyclohexene, 4-methyl-1-(1-methylethyl) (10369); 4-isopropylbenzyl alcohol (325); Selina dien-6alpha-ol (91746575); hydroxycaryophyllene (91747230); tetramethyl-5, 6, 7, 8-tetrahydro-4h-3a,7-methanoazulene (74819450); hydroxyl-dimethyl tetrahydro - 1h-naphthalen - 2 - one (11651583); 1-methyl-5-methylidene-9-propan-2-yltricycloene (91748745); calamenone (5316902); octahydro-1, 4-dimethyl-7-(1-methylethylidene) azulene monoepoxide (162213); scoparone (8417); 4-methoxybenzoic acid (7478); geranylacetone (1549778); 1-hexene (11597); 1-butanol (263); 1-pentadecene (25913); 1-hexen-3-ol (20928); 6-methyl-5-hepten-2-one (9862); ethyl acetate (8857); alpha-guaiene (5317844); delta-guaiene (94275); benzyl benzoate (2345); (+)-delta-selinene (12308846); valencene (9855795); acetone (180); geraniol (637566); 1-tridecene (17095); Undecane (14257); 2,3-butanediol (262); dehydroascorbic acid (440667); zingerone (31211); d-tartaric acid (439655); jasmonic acid (5281166); vomifoliol (5280462); ethyl butyrate (7762); damascenone (5366074); methyl anthranilate (8635); dehydrovomifoliol (688492); oxalic acid (971); ethyl 3-hydroxybutyrate (62572); grasshopper ketone (13922639); cis-2-hexen-1-ol (5324489); citronellol (8842); methyl vanillate (19844); nerol (643820); 1-(4-hydroxy-3-methoxyphenyl) propan-1-one (15782); 2,3-dimethoxyphenol (78828); tartarate (3806114); calamenene (6429077); dihydrozeatin (32021); ethyl decanoate (8048); methyl 3-hydroxybutyrate (15146); ethyl trans-4-decenoate (5362583); catechol (289); alpha-terpineol (17100); trans-zeatin (449093); benzyl alcohol (244); decanoic acid (2969); 5-hydroxymethylfurfural (237332); octanoic acid (379); 4-ethylphenol (31242); 2-methoxy-4-vinylphenol (332); eugenol (3314); acetovanillone (2214); furfuryl alcohol (7361); phenylacetaldehyde (998); 4-ethyl-2-methoxyphenol (62465); 2,6-dimethoxyphenol (7041); d-limonene (440917); 1,3-propanediol (10442); trans-stilbene (638088); resveratrol (445154); propanol (1031); 2,6-dimethyl-7-octene-2,3,6-triol (15241411); 5-ethoxydihydro-2(3h)-

furanone (356063); ethyl hexanoate (31265); isoamyl acetate (31276); (6e)-8-hydroxygeraniol (5363397); 1-(+)-arabinose (439764); vitispirane (6450832); piceatannol (667639); ethyl dodecanoate (7800); ethyl octanoate (7799); alpha-damascenone (68473438); isobutanol (6560); d-fructose (2723872); l-rhamnose (25310); ethyl lactate (7344); isobutyramide (68424); pellitorine (5318516); dehydro-alpha-lapachone (72734); lapachol (3884); mannitol (6251); 3h-naphtho (1,8-bc) furan-3,8(4h)-dione,5,5a,6,7-tetrahydro-7-methyl-5-1-methylethyl (156117); isobutyl butyrate (10885); isovaleric acid (10430); 3-octanol (11527); methyl salicylate (41330); methyl tetradecanoate (31284); 2,4-decadienal (5283349); 2-nonenal (5283335); hexyl butyrate (17525); 2-methylbutyl 2-methylbutyrate (1712); 2-methylbutyl butyrate (162627); 2-undecenal (5283356); 2-octenal (5283324); methyl benzoate (7150); 1-dodecanol (8193); hexadecanal (984); butyl butyrate (7983); 4-ethyl-2-methoxyphenol (62465); 1-heptanol (8129); phenethyl isovalerate (8792); 1-heptadecene (23217); butyric acid (264); ethyl isovalerate (7945); ethyl Salicylate (8365); cis-3-hexenyl acetate (5363388); nonanoic acid (8158); 2-tetradecenal (5283366); (e,z)-2,4-decadienal (6427087); 2-methylbutyl isovalerate (62445); cis-3-hexenyl hexanoate (5352543); (z)-3-hexenyl octanoate (5352267); isoxazole (9254); benzoic acid (243); umbelliferone (5281426); methyl 4-methoxycinnamate (641297); l-rhamnose (637542); haplopine (5281846); kokusagine (5318829); gamma-fagarine (107936); marmesin (334704); aegelinol (600671); methoxsalen (4114); bergapten (2355); psoralen (6199); xanthotoxol (65090); isopimpinellin (68079); dictamnine (68085); 4-isopropylbenzaldehyde (326); trans-1(7); 8-p-menthadien-2-ol (6428442); halfordinol (80048); myrtenyl acetate (61262); methyloxabicycloheptane (10953718); citral (638011); alpha-phellandrene (443160); citronellal (7794); p-menth-1-en-3-ol (10282); aristolene (530421); beta-ocimene (5320250); trimethyl-4-methylenedecahydro-1h cyclopropanal (522266); cis-sabinol (94147); isoaromadendrene epoxide (534398); longipinocarveol, trans (534645); 2-cyclopenten-1-one, 2-(2-butenyl)-3-methyl (5373127); methyl-2-octenedial (5370208); 5-isopropenyl-2-methyl-2-cyclohexenyl pivalate (545235); 4-allyltoluene (76851); 3-fluorophenyl

cyclohexanecarboxylate (53401233); 5-isopropyl-6-methyl-hepta-3,5-dien-2-ol (5363138); 1-benzoxirene-2,5-dione, 4-(3-oxobutyl) hexahydro-3,3,4-trimethyl (536547); 2,3-pinandiol (62044); l-arabinose (439195); osthole (10228); 3-octanone (246728); eugenol (92349); halfordinol (442858); dimethyl terephthalate (8441); harmaline (442118); harmine (5280953); harmol (68094); harmalol (3565); harman (5281404); 9h-pyrido[3,4-b]indole (64961); n,n-dimethyl-5-methoxytryptamine (1832); candicine (23135); n,n-dimethyltryptamine (6089); hordenine (68313); n-methyltyramine (9727); n-methyltetrahydroharman (68741157); 9h-pyrido[2,3-b] indole (67486); methyl 1-methoxy-1h-indole-3-carboxylate (10465540); tryptamine (1150); caffeic acid (689043); benzophenone (3102); 2-(3-methylphenyl) propan-2-ol (255195); 2-nitrophenol (6947); tetramethyltricycloundec-9-ene (91753627); myrtenal (61130); gamma-pinene (6431006); 5-isopropylbicyclo [3.1.0] hexan-2-one (92784); methylcyclopentane (7296); aromadendrene (11095734); fenchol (15406); isopentyl benzoate (7193); hexyl benzoate (23235); 2-[2(dimethylamino) ethylsulfanyl] naphthalene-1,4-dione (428289); verbenol (61126) (+)-trans-piperitenol (855682-cyclohexen-1-ol, 3-methyl-6-(1-methylethyl)-, (1r,6s)-rel- (85567); toluene (1140); (z)-gamma-bisabolene (3033866); alpha cubebene (442359); acoradiene (90351); (z)-alpha-bisabolene (5352653); methyl 4-methoxybenzoate (8499); (1s,2s,6s,7r,8r)-1,3-dimethyl-8-propan-2-yltricyclo[4.4.0.02,7] dec-3-ene (101607926); junenol (6452077); ascaridole (10545); thujyl alcohol (10550); isocineole (10106); selina-4(15);7(11)-diene (10655819); methyl geranate (5365910); (e)-4,8-dimethyl-1,3,7-nonatriene (6427110); perillene (68316); terpinene 4-acetate (20960); tagetonol (522417); geranyl acetate (1549026); neryl acetate (1549025); acetylcholine (187); sabinene hydrate (62367); trans-pinocarveol (88302); (+)-isomenthol (45056); ledol (92812); 2-heptene (11611); germacrene b (5281519); citronellyl propionate (8834); (e)-gamma-bisabolene (5352437); farnesol (445070); hex-2-en-3-ol (22227611); 1-nonen-3-ol (89560); terpiryl acetate (91691738); menthone (26447); beta-d-xylopyranose (125409); l-vasicinone (442935); scopoletin (5280460); cinnamaldehyde (637511); copaene (12303902); carotol (442347); gamma-terpineol (11467); methyl salicylate (4133);

coumarin (323); tetradecanal (31291); cinnamyl acetate (5282110); safrole (5144); cinnamyl alcohol (5315892); phenethyl acetate (7654); thymol (6989); ethyl benzoate (7165); 2-hydroxy-3-phenylprop-2-enal (71407359); acetyleugenol (7136); estragole (8815); 4'-methylacetophenone (8500); carvacrol methyl ether (80790); 4-allylphenol (68148); beta-cubebene (93081); citronellyl acetate (9017); citronellyl butyrate (8835); cubenene (57357909); 2,10-epoxypinane (93046); eucalyptol (2758); geranyl propionate (5355853); phenethyl benzoate (7194); neryl propionate (5365982); germacrene d (5317570); dl-borneol (64685); cinnamic acid (444539); cis-cinnamaldehyde (6428995); alpha-ylangene (442409); alpha-bergamotene (86608); (+)-endo-beta-bergamotene (12300073); levomenol (442343); bornyl acetate (93009); cis-sabinene hydrate (20055523); cubenol (11770062); menthol (1254); cyclohexane (8078); ethylidene diacetate (222536); methoxycinnamaldehyde (4452795); 2-methoxycinnamaldehyde (641298); beta-guaiene (6949); (z)-cinnamyl acetate (5315912); tricyclene (79035); beta-farnesene (5281517); 10-epi-eudesmol (6428994); alpha-fenchol (439711 epi-cubenol (12046149); bisabolol (1549992); alpha-muurolol (91753440); o-cymene (10703); octanal (454); carvacrol (10364); elemicin (10248); mintsulfide (14564587); bicyclogermacrene (13894537); cis-3-hexenal (643941); 2-heptanone (8051); geranyl formate (5282109); styrene (7501); linalyl propionate (61098); isosafrole (637796); geranyl tiglate (5367785); isospathulenol (14038848); nonan-1-ol (8914); (z)-beta-ocimenol (91753567); viridiflorene (10910653); zingiberenol (13213649); 2-nonanol (12367); cis-3-hexenyl benzoate (5367706); cis-linalool oxide (6428573); piperitone (6987); phenethyl anthranilate (8615); 2-phenylethyl propionate (31225); 6-camphenol (180537); cyclocolorenone (160491); decane (15600); 2,3-dimethylstyrene (33936); acorenone b (21674978); (1s)-(+)-menthyl acetate (62335); isobutyric acid (6590); delta-terpineol (81722); 14-hydroxy-9-epi-(e)-caryophyllene (5352484); isoamyl isovalerate (12613); 2-isopropyl-1-methoxy-4-methylbenzene (161716); cis-4-hydroxy-L-proline (440015); D-glucose (5793); alpha-santalene (94164); gamma-curcumen (12304273); alpha-bergamotenol (5368743); (z)-lanceol (15560069); bisabolenol (91747530);

campherene-2,13-diol (42608198); alpha-santaldiol (44583958); beta-santaldiol (15276127); (z)-.beta.-curcumen-12-ol (91710638); (z)-gamma-curcumen-12-ol (91747459); santene (10720); bornylene (10047); (e)-.alpha.-santallic acid (14059029); 3-methylbutanal (11552); himachalol (121536); exo-norbicycloekasantalal (85320720); (-)-beta-curcumen (14014430); germacrene c (25244915); alpha santalol (11085337); (e)-alpha-bisabolene (5315468); alpha-ocimene (5320249); alpha-teresantallic acid (5321816); teresantalol (578221); cis-lanceol (6536796); 2-carene (79044); cuparene (86895); beta-terpinene (66841); trans-isolongifolanone (6427070); beta-santallic acid (131752692); beta-oplopenone (14038847); cis-nuciferol (6430906); epi-beta-santalene (11106484); beta-santalol (6857681); (z)-.beta.-santalol (5281532); epi-globulol (7308311); norecasantallic acid (100966488); bergamotene (521569); 3-(4-methylcyclohex-3-en-1-yl) butanal (110923); 1-furfurylpyrrole (15037); sesquisabinene (25202482); beta-santalal (101449606); 2-methoxy-4-methylphenol (7144); dendrolasin (5316534); 4-vinylphenol (62453); isodihydroagarofuran (10775429); fokienol (5352449); cedr-8-ene (6431015); sorbitol (5780); phenanthrene (995); 9,10-dihydro-2,3,5,7-phenanthrenetetrol (22753774); 2,4,5,6-phenanthrenetetrol (129206075); calcium oxalate (33005); saccharin (5143); eugenin (10189); 2-hexanone (11583); vanillin (1183); myristicin (4276); 2- isoeugenitol (5318562); propyl benzoate (16846); palustrol (110745); acetophenone (7410); benzyl salicylate (8363); thymol acetate (68252); isoeugenol (853433); alpha-asarone (636822); isocaryophyllene (5281522); fenchone (14525); alpha-humulene epoxide (14038843); gamma-cadinene (92313); humuladienone (101297706); methyl acetate (6584); heptadecane (12398); naphthalene (931); butyl benzoate (8698); pulegone (442495); ethylene glycol dimethacrylate (7355); 1-(furan-2-yl)ethanol (107243); 5-methylfurfural (12097); 2-heptyl benzoate (243678); 1-methylhexyl acetate (80018); pentanal (8063); gamma-decalactone (12813); 1-methyloctyl acetate (85788); tetracyclo [6.3.2.0(2,5).0(1,8)] tridecan-9-ol (585744); 2-hydroxy-4-oxoisophorone (37246); 2, 2, 6-trimethylcyclohexane-1,4-dione (30181); safranal (61041); isophorone (6544); 2,6,6-trimethyl-2-cyclohexene-1,4-dione (62374);

salicylic acid (338); 2-butenic acid (637090); benzyl alcohol (244); isoamyl alcohol (31260); 4-hydroxy-2, 6, 6-trimethyl - 3 - oxo-1, 4-cyclohexadiene-1-carboxaldehyde (15715950); (3s)-3-hydroxycyclocitral (25201359); 4-hydroxy-3,5,5-trimethylcyclohex-2-enone (566734); xanthone (7020); 1,4-benzoquinone(4650); d-galacturonic acid (439215); galactaric acid (3037582); methyl gallate (7428); nicotinic acid (938); phloroglucinol (359); phyllantidine (12314211); quercitol (441437); (-)-anaferine (443143); cuscohygrine (1201543); esculetin (5281416); galactitol (11850); gamma-aminobutyric acid(119); hygrine (440933); myristic acid (11005); nicotine (89594); pelletierine (92987); tropine (449293); withasomnine (442877); 1-undecanol (8184); biotin (171548); d-glucuronic acid (94715); d-xylose (135191); farnesal (5280598); nerolidol (5284507); pantothenic acid (6613);(+)-alpha-gurjunene (15560275); 4'-methoxyacetophenone (7476); alpha-terpinyl acetate(111037); camphene (6616); decanal (8175); delta-elemene(12309449); dodecanal (8194); hexadecane (11006); tridecane (12388); zingiberene (92776). 5-hexen-2-one (7989); 1-methylcyclohexene (11574); dihydroxyxanthone (5493674); 1,4-dimethoxybenzene (9016); 2-decanone (12741); 3-methyl-2-pentanone (11262); 4-acetyl-1-methylcyclohexene (93019); drima-7,9-diene (6429215); myristoleic acid (5281119); 2-pentadecenoic acid (5282742); 1-hydroxy-7-methoxyxanthone (12214329); 1,5,6-trihydroxyxanthone (5281652); euxanthone (5281631); 1,5-dihydroxyxanthone (5480299); beta-acoradiene (5316209); 6-methyl-3, 5-heptadien-2-one (5370101); ferruxanthone (129636605); (1r,4r,4ar,6s,8ar)-1,6-dimethyl-4-propan-2-yl-3, 4, 4a, 5, 6, 7, 8, 8a-octahydro-2h-naphthalen-1-ol (100949538); 2-decenal (5283345); n-trans-cinnamoylimidazole (5357650); methyl 4-vinylbenzoate (583124); 4-methyl-2-phenyl-1,3-dioxolane (595928); cadalene (10225); sativene (11830550); 3-phenylpropyl acetate (31226); 4-methoxybenzaldehyde (31244); geranyl butyrate (5355856); citronellylformate (7778); salicylaldehyde (6998); 2-methoxybenzaldehyde (8658); 3-phenyl-1-propanol (31234); 3-phenylpropanal (7707); p-mentha-1,3,8-triene (176983); p-menthan-3-one (6986); cubenol (519857); methyl-3-propan-2-ylcyclohexane

(27938); isobornyl acetate (6950273); isospathulenol (102303030); methyl cinnamate (6428458); dihydrocarveol (12072); sesquiphellandrene (519764); alloocimene (5368821); dihydrolinalool (86749) and 2-cyclohexen-1-ol(122484).

The corresponding three-dimensional structures of these molecules were retrieved from the PubChem database to enable molecular docking and related computational studies. To assess their pharmacokinetic and safety profiles, all selected ligands were subjected to screening of Absorption, Distribution, Metabolism, Excretion, and Toxicity (ADMET).

This step ensures the identification of compounds with favorable drug likeness and bioavailability, thereby narrowing the list to those best suited for further docking and interaction studies with targets.

Lead Compound Selection: Phytochemicals from 41 medicinal plants and three reference drugs were evaluated for pharmacokinetic and physicochemical properties using the SwissADME tool ⁹. Parameters such as molecular weight, HBD, HBA, TPSA, LogS, GI absorption, and BBB permeability were assessed.

Drug-likeness was determined *via* Lipinski's Rule of Five, with a molecular weight cutoff of ≤ 250 g/mol to prioritize BBB-permeable compounds. Selected candidates were further analyzed for toxicity using the ProTox-II v3.0 platform ¹⁰, assessing acute oral toxicity, organ toxicity, and carcinogenicity. Seven compounds with favorable ADMET profiles and safety margins were identified as leads for molecular docking and advanced computational studies.

Target Selection and Retrieval: The selected HMPV targets play critical roles in viral replication and pathogenesis were retrieved from the Protein Data Bank. The N-P complex (5FVD) facilitates genome encapsidation and polymerase recruitment ¹¹.

The prefusion-closed trimer of the F protein (8W3Q) and prefusion trimer (8VT3) mediate viral entry by enabling membrane fusion and are key targets for neutralizing antibodies ¹². The M2-1 tetramer (4CSA) acts as a transcriptional

antiterminator, enhancing RNA polymerase processivity¹³. The polymerase phosphoprotein complex (6U5O) constitutes the viral replication machinery¹⁴, where the P protein anchors and stabilizes the L polymerase on the nucleocapsid¹⁵. These proteins are essential for maintaining HMPV's structural integrity and supporting its transcriptional and replicative functions.

Molecular Docking and Interaction Analysis:

Prior to docking, all targets and ADMET passed ligands were prepared using PyRx, which facilitated energy minimization and conversion of ligands to the appropriate PDBQT format. Protein structures were refined by removing nonessential heteroatoms and adding polar hydrogens.

Molecular docking was carried out by defining target specific grid box coordinates tailored to the predicted active sites of five key HMPV protein targets. The grid centers were configured as follows: polymerasephosphoprotein complex at X: 80.58, Y: 100.71, Z: 83.06; prefusion closed trimer at X: 86.70, Y: 57.82, Z: 52.06; M2-1 tetramer at X: 70.12, Y: 56.00, Z: 94.59; prefusion trimer at X: 64.34, Y: 70.58, Z: 126.86; and the N-P complex at X: 52.69, Y: 87.96, Z: 80.30.

These coordinates were employed in the PyRxintegrated AutoDock Vina platform to construct receptorspecific docking grids, enabling precise ligand orientation and reliable interaction profiling within the functional binding regions^{16,17}. Postdocking, binding affinities were recorded, and docked complexes were visualized and analyzed using BIOVIA Discovery Studio Visualizer to identify key molecular interactions, such as hydrogen bonds and hydrophobic contacts¹⁸.

RESULTS AND DISCUSSION:

Bioavailability and Toxicity Assessment:

Phytochemicals from 41 medicinal plants, along with three FDA approved drugs; Ribavirin, Penicillin V and Ibuprofen, were evaluated for their pharmacokinetic, physicochemical, and toxicity profiles using SwissADME and ProTox-II platforms. Initial screening identified seven phytochemicals; Isobutyric acid, 3-methylbutanal, Isoamyl alcohol, Isovaleric acid, Propanoic acid, Butyric acid, and 1-butanol, that exhibited favorable ADMET characteristics.

All selected phytochemicals had molecular weights below 110 g/mol, placing them within an optimal range for blood brain barrier (BBB) permeability and oral bioavailability.

They also complied with Lipinski's Rule of Five, based on parameters such as hydrogen bond donors and acceptors, rotatable bonds, and topological polar surface area (TPSA), indicating strong drug likeness^{19,20}.

Each compound showed high gastrointestinal (GI) absorption and was predicted to cross the BBB, an important attribute for targeting viral infections. None of the compounds were P-glycoprotein substrates and CYP450 inhibitors, suggesting minimal risk of efflux issues.

Bioavailability scores ranged from 0.55 to 0.85, and toxicity analysis confirmed all were non-toxic, with no evidence of acute toxicity, organ damage and carcinogenicity. Among them, Propanoic acid and 1-butanol emerged as the most promising, due to their low molecular weights, excellent solubility, and high oral bioavailability, making them strong candidates for further docking studies.

To provide reference standards, Ribavirin, Ibuprofen and Penicillin V were also analyzed. While three complied with Lipinski's rules, only Ibuprofen demonstrated BBB permeability. Despite good GI absorption, Penicillin V's higher molecular weight and TPSA likely limited its systemic circulation. Three drugs showed predicted toxicity, aligning with known clinical profiles. The ADMET profiles of the selected phytochemicals and the three FDA approved reference drugs are presented in the table-1 and supplementary datatable-1.

These observations not only reaffirm their therapeutic value and pharmacological limitations, but also underscore the importance of comprehensive ADMET profiling in the early stages of drug discovery. In summary, the comparative evaluation highlights the promising druglikeness and safety of the selected phytochemicals, particularly Propanoic acid and 1-butanol, supporting their further exploration as potential antiHMPV agents.

TABLE 1: ADMET PROFILE OF SELECTED PHYTOCHEMICALS FROM DABUR CHYAWANPRASH AND FDA APPROVED REFERENCE DRUGS

Com. Name	Molecular Formula	Molecular Weight	Rotatable Bonds	H-Acceptor	H-Donor	TP SA	Consensus logP	Solubility	GI Absorption	BBB Permeability	Pgp Substrate	CYP Inhibitors	Lipinski Violation	Bioavailability Score	Toxicity
Ribavirin	C8H12N4O5	244.20	3	7	4	143.7	-2.14	Soluble	Low	No	No	No	Yes	0.55	Yes
Penicillin V	C16H18N2O5S	350.39	6	5	2	121.24	1.15	Soluble	high	no	no	no	0	0.56	Yes
Ibuprofen	C13H18O2	206.28	4	2	1	37.30	3.00	soluble	high	yes	no	no	0	0.85	Yes
Isobutyric acid	C4H8O2	88.11	1	2	1	37.30	0.65	Soluble	High	Yes	No	No	0	0.85	No
3-Methylbutanal	C5H10O	86.13	2	1	0	17.07	1.14	Soluble	High	Yes	No	No	0	0.55	No
Isoamyl alcohol	C5H12O	88.15	2	1	1	20.23	1.16	Soluble	High	Yes	No	No	0	0.55	No
Isovaleric acid	C5H10O2	102.13	2	2	1	37.30	0.98	Soluble	High	Yes	No	No	0	0.85	No
Propanoic acid	C3H6O2	74.08	1	2	1	37.20	0.30	Soluble	High	Yes	No	No	0	0.85	No
Butyric acid	C4H8O2	88.11	2	2	1	37.30	0.68	Soluble	High	Yes	No	No	0	0.85	No
1-Buatanol	C4H10O	74.12	2	1	1	20.23	0.88	Soluble	High	yes	no	no	0	0.55	No

Molecular Docking and Interaction Analysis:

Molecular docking was conducted to assess the binding affinities and interaction profiles of seven ADMET screened phytochemicals and three FDA approved drugs with five key Human Metapneumovirus (HMPV) targets: polymerase phosphoprotein complex, prefusion closed trimer, M2-1 tetramer, prefusion trimer and N-P complex. Docking simulations revealed key ligand-receptor interactions, including hydrogen bonds, hydrophobic, and electrostatic contacts. Binding affinities were calculated and compared to reference drugs. Visualization and structural analysis demonstrated flexibility in receptor active sites, supporting their ability to bind diverse ligands. These findings highlight the potential of selected phytochemicals as promising antiviral agents against HMPV.

Interaction Profile of Reference Leads with Polymerase Phosphoprotein, Prefusion Closed Trimer, M2-1 Tetramer, Prefusion Trimer and N-P complex Target: The molecular docking simulations revealed distinct binding profiles and interaction strengths for the three reference drugs; Ribavirin, Penicillin, and Ibuprofen across five essential HMPV protein targets: the polymerase phosphoprotein complex, prefusion closed trimer, M2-1 tetramer, prefusion trimer, and the N-P complex. Ribavirin, a broad-spectrum antiviral agent, exhibited strong binding affinities with all

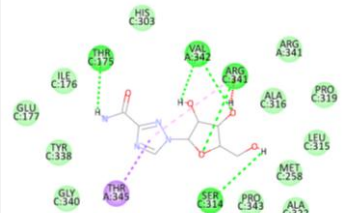
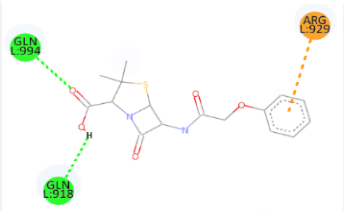
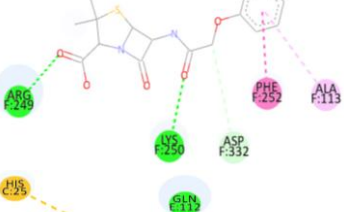
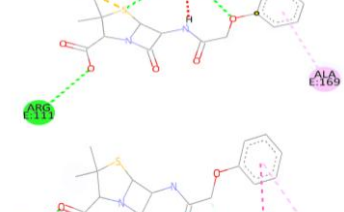

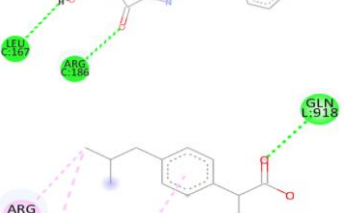
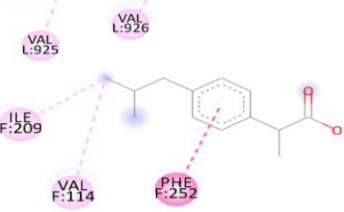
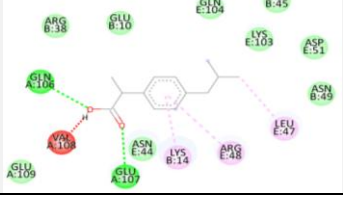

HMPV targets, particularly the M2-1 tetramer (-7.3 kcal/mol) and N-P complex (-7.2 kcal/mol). Notable interactions included hydrogen bonding with critical residues such as Arg-3 and His-25 (M2-1 tetramer), as well as Thr-175, Val-342, Arg-341, and Ser-314 (N-P complex). These residues are implicated in RNA binding and transcriptional regulation, suggesting Ribavirin's potential to disrupt viral transcriptional machinery. However, binding to the prefusion closed trimer was comparatively weaker (-6.0 kcal/mol), with no direct hydrogen bonds detected, indicating limited interaction at this site. Penicillin consistently demonstrated the highest binding affinities among the three drugs, with particularly strong interactions observed with the N-P complex (-7.7 kcal/mol) and prefusion trimer (-7.5 kcal/mol). Key interacting residues included Leu-167, Arg-186, Thr-257, and Arg-260 in the N-P complex, which are known to play crucial roles in nucleocapsid assembly and polymerase recruitment. Similarly, significant interactions with Arg-249 and Lys-250 in both the prefusion trimer and prefusion closed trimer further highlight Penicillin's robust engagement with membrane fusion machinery. The high number of conventional hydrogen bonds formed suggests strong and stable binding, potentially interfering with multiple stages of the viral lifecycle. Ibuprofen, though not an antiviral by design, showed moderate to strong affinities with several

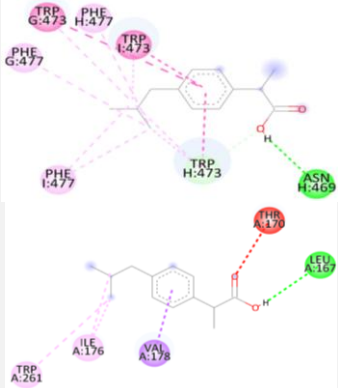
targets, with the prefusion trimer (-7.3 kcal/mol) and M2-1 tetramer (-7.2 kcal/mol) yielding the most favorable scores. Binding residues included Asn-469, Gln-106, and Glu-107, indicative of hydrophilic and electrostatic interactions. However, the binding energy to the polymerase phosphoprotein complex was relatively weak (-5.8 kcal/mol), and no hydrogen bonds were observed with the prefusion closed trimer, suggesting limited therapeutic relevance for Ibuprofen in targeting these sites. Collectively, these results underscore the potential of Penicillin as a multi-target inhibitor with the highest overall binding performance across all viral proteins analyzed, particularly in regions essential for viral replication and fusion. Ribavirin also exhibited promising interaction profiles,

especially with proteins involved in transcriptional regulation. While Ibuprofen displayed moderate binding to selected targets, its lower overall affinity and limited hydrogen bonding interactions suggest it may be less effective as a direct antiviral agent against HMPV. A summary of the results is provided in the **Table 2**. The binding patterns observed in this study offer valuable insights into the molecular determinants of drug-target interactions in HMPV and serve as a foundation for further structure-based optimization of antiviral candidates. Future experimental validation through *in-vitro* and *in-vivo* assays is warranted to confirm the antiviral potential of these reference drugs, particularly Penicillin and Ribavirin, as repurposing candidates against HMPV.

TABLE 2: BINDING AFFINITIES AND KEY HYDROGEN BONDING INTERACTIONS OF REFERENCE DRUGS WITH HUMAN METAPNEUMOVIRUS (HMPV) TARGETS

Reference Drug Name	Receptors	Binding Affinity (Kcal/mol)	Conventional Hydrogen Binding	HMPV Targets Amino Acids 2D Interaction with FDA Approved Drugs
Ribavirin	Polymerase Phosphoprotein Complex	-6.8	Ile-212, Lys-419, Arg-191, Met-211, Thr-192, Gly-188, Arg-191	
	Prefusion Closed Trimer	-6.0	-	
	M2-1 Tetramer	-7.3	Arg-3, His-25	
	Prefusion Trimer	-6.7	Gln-307, Glu-305, Asn-457, Leu-105, Lys-362	

Penicillin	N-P Complex	-7.2	Thr-175, Val-342, Arg-341, Ser-314	
	Polymerase Phosphoprotein Complex	-6.9	Gln-918, Gln-994	
	Prefusion Closed Trimer	-6.8	Arg-249, Lys-250	
	M2-1 Tetramer	-7.5	Arg-111, Gln-112	
	Prefusion Trimer	-7.5	Arg-249, Lys-250	
Ibuprofen	N-P Complex	-7.7	Leu-167, Arg-186, Thr-257, Arg-260	
	Polymerase Phosphoprotein Complex	-5.8	Gln-918	
	Prefusion Closed Trimer	-6.7	-No-	
	M2-1 Tetramer	-7.2	Gln-106, Glu-107	

Prefusion Trimer	-7.3	Asn-469	
N-P Complex	-6.4	Leu-167	

Interaction Profiling of Phytochemicals with Polymerase Phosphoprotein Target: The binding interactions of the selected compounds with the polymerase phosphoprotein target were analyzed to evaluate their affinities and molecular interaction profiles. Isovaleric acid demonstrated the highest binding affinity at -4.5 kcal/mol, forming stable hydrogen bonds with Gln-567, Ala-476, and Arg-572, indicating a strong and favorable interaction. Isobutyric acid and butyric acid each showed moderate binding affinities of -4.1 kcal/mol. Isobutyric acid interacted with Ser-930, Ser-1277, Gln-1326, and Ser-1322, while butyric acid engaged with Tyr-17, Ser-16, and Trp-827, suggesting robust multiresidue interactions. Propionic acid, also with a binding affinity of -4.1 kcal/mol, primarily formed interactions with Glu-383 and Arg-208. Isoamyl alcohol, with a binding energy of -3.9 kcal/mol, showed interactions involving Asn-829, Trp-827, and Thr-830, reflecting a combination of polar and aromatic contacts. Comparatively, 3-methylbutanol and 1-butanol exhibited lower binding affinities of -3.7 and -3.6 kcal/mol, respectively, yet maintained key interactions with residues such as Arg-209, Thr-385, Thr-830, and Trp-827. The obtained results are curated in the **Table 3**. These findings highlight variable binding strengths among the compounds and emphasize the potential of isovaleric acid as a lead candidate for further investigation.

Interaction Profiling of Phytochemicals with Prefusion Closed Trimer Target: The polymerase prefusion closed trimer exhibited varying binding affinities with the tested compounds, reflecting distinct interaction profiles. Butyric acid displayed a binding affinity of -4.3 kcal/mol, forming interactions with Asp-332 and Lys-250, indicative of both electrostatic and hydrogen bond

interactions. Isoamyl alcohol showed a slightly lower binding affinity of -3.8 kcal/mol, engaging primarily with Gly-251 and Pro-211, residues typically associated with hydrophobic interactions. Isobutyric acid and isovaleric acid exhibited binding affinities of -4.0 and -4.2 kcal/mol, respectively, interacting with Leu-66, Ile-67, and Ser-65, suggesting stable contacts within the hydrophobic core of the binding site. Similarly, propanoic acid, with a binding energy of -4.2 kcal/mol, interacted with Cys-178, Leu-66, Ile-67, and Ser-65, reinforcing the trend of favorable interactions involving small, hydrophobic ligands. The results are summarized in table-3. Collectively, these results suggest a binding site preference for low molecular weight, hydrophobic compounds, particularly isobutyric and propanoic acids, based on both residue engagement and docking energies.

Interaction Profiling of Phytochemicals with M2-1 Tetramer Target: The M2-1 tetramer exhibited distinct binding preferences among the tested compounds. Butyric acid demonstrated the highest binding affinity at -4.7 kcal/mol, forming interactions with key residues such as Tyr-27, Asn-44, Val-108, Glu-107, and Gln-106. This extensive interaction profile suggests the involvement of multiple hydrogen bonds and hydrophobic contacts, indicating a highly stable binding mode. Isovaleric acid and isobutyric acid followed closely, with binding affinities of -4.6 and -4.4 kcal/mol, respectively, engaging residues like Asp-51, Arg-48, Gln-45, Glu-10 followed by Tyr-27, Glu-107, Gln-106, Val-108. Isoamyl alcohol displayed a moderate binding energy of -4.1 kcal/mol, interacting with His-25, Arg-3, and Phe-23. In contrast, propionic acid showed the weakest binding affinity of -3.8 kcal/mol, with limited interactions involving Lys-103, Asn-49, Arg-48,

and Gln-45. A summary of the results is provided in the table-3. Overall, the M2-1 tetramer receptor displayed a higher affinity for compounds such as butyric acid and isovaleric acid, which engaged multiple residues and demonstrated more stable interaction profiles, highlighting their potential as lead candidates for targeting this viral protein.

Interaction Profiling of Phytochemicals with Prefusion Trimer Target: The prefusion trimer demonstrated variable binding affinities across the tested compounds. Isoamyl alcohol and isobutyric acid exhibited moderate binding energies of -4.1 and -3.9 kcal/mol, respectively, primarily interacting with the hydrophobic residue Trp-473. Isovaleric acid showed a higher binding affinity of -4.4 kcal/mol; however, no specific interacting residues were identified in the docking output, possibly due to transient contacts. Interestingly, propionic acid, despite a lower affinity of -3.7 kcal/mol, formed multiple interactions with residues including Leu-105, Gly-106, Asn-457, Tyr-319, and Glu-305, suggesting a more distributed binding pattern. 1-Butanol displayed the lowest binding energy of -3.4 kcal/mol, primarily engaging Tyr-310. The key results are consolidated in table-3The overall interaction profile highlights the receptor’s preference for hydrophobic ligands,

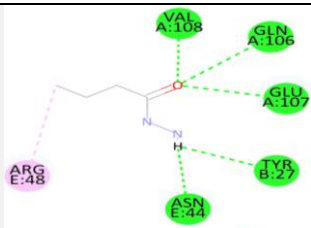
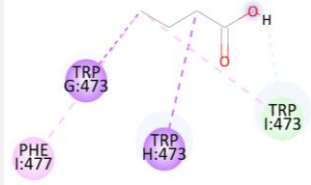

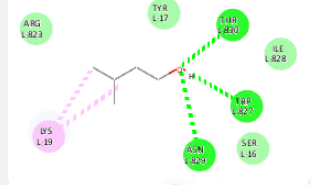
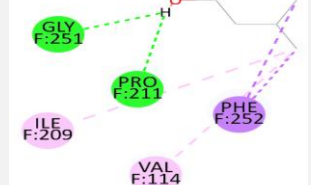
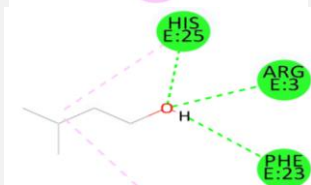
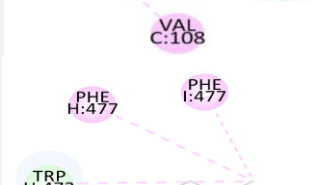
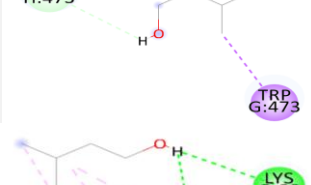
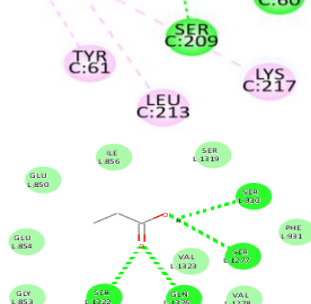
particularly those interacting with residues like Trp-473 and Tyr-310, suggesting that larger, nonpolar compounds such as isovaleric acid and isoamyl alcohol may be better suited to engage this binding pocket effectively.

Interaction Profiling of Phytochemicals with N-P complex Target: The N-P complex exhibited binding affinities ranging from -3.5 to -4.4 kcal/mol across the tested compounds. 1-Butanol and propionic acid showed the weakest binding energies (-3.5 kcal/mol), interacting with residues such as Arg-132. Isoamyl alcohol and isobutyric acid demonstrated moderate binding affinities (-4.0 kcal/mol), engaging key residues including Lys-60, Ser-209, and Arg-341. Isovaleric acid exhibited the strongest interaction with a binding affinity of -4.4 kcal/mol, forming stable contacts with Lys-60, Glu-64, and additional surrounding residues. The main outcomes are detailed in table-3These findings suggest that the receptor favors longerchain, hydrophobic, ligands, particularly those capable of interacting with charged or polar residues. Overall, the receptor demonstrates the flexibility to accommodate a range of small molecules, with isovaleric acid emerging as the most promising candidate based on binding strength and interaction profile.

TABLE 3: PREDICTED BINDING AFFINITIES AND KEY HYDROGEN BONDING INTERACTIONS OF ADMET-SCREENED PHYTOCHEMICALS WITH HUMAN METAPNEUMOVIRUS (HMPV) TARGETS

Phyto Chemical Name	Receptors	Binding Affinity (Kcal/mol)	Conventional Hydrogen Binding	HMPV Targets Amino Acids 2D Interaction with Phyto Chemicals
1-Butanol	Polymerase Phosphoprotein Complex6U5O	-3.6	Thr-830, Trp-827	
	Prefusion Closed Trimer8W3Q	-3.6	Leu-298	
	M2-1 Tetramer4CSA	-3.6	Gln-104, Tyr-9	

	Prefusion Trimer8VT3	-3.4	Tyr-310	
	N-P Complex5FVD	-3.5	Arg-132	
3-methyl butanol	Polymerase Phosphoprotein Complex6U5O	-3.7	Arg-209, Thr- 385	
	Prefusion Closed Trimer8W3Q	-3.8	Arg-300	
	M2-1 Tetramer4CSA	-4.0	Val-108, Gln- 106, Glu-107	
	Prefusion Trimer8VT3	-4.2	-	
	N-P Complex5FVD	-3.6	Ser-209, Ala- 63, Glu-64	
Butyric acid	Polymerase Phosphoprotein Complex6U5O	-4.1	Tyr-17, Ser-16, Trp-827	
	Prefusion Closed Trimer8W3Q	-4.3	Asp-332, Lys- 250	

Isoamyl alcohol	M2-1 Tetramer4CSA	-4.7	Tyr-27, Asn-44, Val-108, Glu-107, Gln-106	
	Prefusion Trimer8VT3	-3.6	-	
	N-P Complex5FVD	-3.7	Asp-58, Ala-57	
	Polymerase Phosphoprotein Complex6U5O	-3.9	Asn-829, Trp-827, Thr-830	
	Prefusion Closed Trimer8W3Q	-3.8	Gly-251, Pro-211	
	M2-1 Tetramer4CSA	-4.1	His-25, Arg-3, Phe-23	
	Prefusion Trimer8VT3	-4.1	-	
	N-P Complex5FVD	-4.0	Lys-60, Ser-209	
Isobutyric acid	Polymerase Phosphoprotein Complex6U5O	-4.1	Ser-930, Ser-1277, Gln-1326, Ser-1322	

	Prefusion Closed Trimer8W3Q	-4.0	Leu-66, Ile-67, Ser-65	
	M2-1 Tetramer4CSA	-4.4	Asp-51, Arg-48, Gln-45	
	Prefusion Trimer8VT3	-3.9	-	
	N-P Complex5FVD	-4.0	Arg-341	
Isovaleric acid	Polymerase Phosphoprotein Complex6U5O	-4.5	Gln-567, Ala-476, Arg-572	
	Prefusion Closed Trimer8W3Q	-4.2	Cys-178, Leu-66, Ile-67, Ser-65	
	M2-1 Tetramer4CSA	-4.6	Glu-10, Tyr-27, Glu-107, Gln-106, Val-108	
	Prefusion Trimer8VT3	-4.4	-	
	N-P Complex5FVD	-4.4	Lys-60, Glu-64	
Propionic acid	Polymerase Phosphoprotein Complex6U5O	-4.1	Glu-383, Arg-208	

Prefusion Closed Trimer8W3Q	-4.2	Cys-178, Leu-66, Ile-67, Ser-65	
M2-1 Tetramer4CSA	-3.8	Lys-103, Asn-49, Arg-48, Gln-45	
Prefusion Trimer8VT3	-3.7	Leu-105, Gly-106, Asn-457, Tyr-319, Glu-305	
N-P Complex5FVD	-3.5	Val-342, Ala-316, Arg-341	

CONCLUSION: This study provides a comprehensive *in-silico* evaluation of bioactive phytochemicals from the Ayurvedic formulation Dabur Chyawanprash, along with three FDA approved reference drugs, focusing on their pharmacokinetic properties, toxicity profiles, and molecular docking interactions with five key HMPV protein targets. ADMET analysis revealed that all selected phytochemicals possess favorable druglike characteristics, including low molecular weight, high GI absorption, BBB permeability, nontoxic profiles, with none identified as CYP450 inhibitors and P-glycoprotein substrates. Notably, propanoic acid and 1-butanol demonstrated optimal oral bioavailability and safety, emerging as strong candidates for antiviral development. Docking simulations underscored the superior binding efficacy of Ribavirin and Penicillin, which consistently showed the highest affinities across all viral receptors, particularly the N-P Complex (-7.7 kcal/mol) and Prefusion Trimer (-7.5 kcal/mol), forming multiple stable hydrogen bonds. Among phytochemicals, isovaleric acid exhibited the strongest interaction with the polymerase phosphoprotein (-4.5 kcal/mol) and M2-1 tetramer (-4.6 kcal/mol), while butyric acid showed pronounced binding to the M2-1 tetramer (-4.7

kcal/mol). The prefusion closed trimer and prefusion trimer receptors demonstrated a preference for small, hydrophobic ligands such as isobutyric and isoamyl alcohol, suggesting a structural fit within their binding pockets. Overall, the combined ADMET and docking results validate the therapeutic promise of specific short chain fatty acids and alcohols, particularly isovaleric acid and propanoic acid, as potential antiviral agents against HMPV. These findings support further *in-vitro* and *in-vivo* validation and underscore the value of integrating computational tools in early phase drug discovery to identify lead molecules with desirable pharmacological and safety profiles.

ACKNOWLEDGMENT: The authors gratefully acknowledge the management of Indian Academy Institutions for providing the infrastructure and support essential for the successful execution of this study. We also extend our heartfelt thanks to Ms. Chandana and Ms. Nikshitha for their consistent support, insightful suggestions, and valuable assistance at various stages of the research.

Supplementary Data: The complete list of pharmacokinetic and toxicity profiles of selected

phytochemicals available as supplementary data (Supplementary **Table 1**, <https://doi.org/10.5281/zenodo.16326701>).

CONFLICT OF INTEREST: None

REFERENCES:

- Papenburg J and Boivin G: The human metapneumovirus: A newly described respiratory pathogen. *Pediatric Infectious Disease Journal* 2010; 29(2): 134-140. <https://doi.org/10.1097/INF.0b013e3181c1628b>
- Van den Hoogen BG, De Jong JC, Groen J, Kuiken T, De Groot R, Fouchier RA and Osterhaus AD: A newly discovered human pneumovirus isolated from young children with respiratory tract disease. *Nature Medicine* 2001; 7(6): 719-724. <https://doi.org/10.1038/89098>
- Battles MB and McLellan JS: Respiratory syncytial virus and human metapneumovirus. Structure, function, and antigenicity. *Current Opinion in Virology* 2019; 34: 97-106. <https://doi.org/10.1016/j.coviro.2019.01.004>
- Cox RG, Livesay SB and Williams JV: The human metapneumovirus fusion protein mediates entry via an interaction with RGD-binding integrins. *Proceedings of the National Academy of Sciences* 2012; 109(17): 7098-7103. <https://doi.org/10.1073/pnas.1117566109>
- Lionta E, Spyrou G, Vassilatis DK and Cournia Z: Structure-based virtual screening for drug discovery: principles, applications and recent advances. *Current Topics in Medicinal Chemistry* 2014; 14(16): 1923-1938. <https://doi.org/10.2174/1568026614666140929124445>
- Atanasov AG, Waltenberger B and Wenzig EM: Discovery and resupply of pharmacologically active plant-derived natural products: A review. *Biotechnology Advances* 2015; 33(8): 1582-1614. <https://doi.org/10.1016/j.biotechadv.2015.08.001>
- Balasubramani SP, Venkatasubramanian P and Patwardhan B: Ancient but evidence-based: Traditional use and modern phytopharmacology of Ayurvedic Rasayana formulation, Chyawanprash. *Journal of Ethnopharmacology* 2011; 142(3): 593-602. <https://doi.org/10.1016/j.jep.2012.05.009>
- Mohanraj K, Karthikeyan BS and Vivek Ananth RP: IMPPAT: A curated database of Indian Medicinal Plants, Phytochemistry and Therapeutics. *Scientific Reports* 2018; 8: 4329. <https://doi.org/10.1038/s41598-018-22631-z>
- Daina A, Michielin O and Zoete V: SwissADME: a free web tool to evaluate pharmacokinetics, drug-likeness and medicinal chemistry friendliness of small molecules. *Scientific Reports* 2017; 7: 42717. <https://doi.org/10.1038/srep42717>
- Banerjee P, Eckert AO, Schrey AK and Preissner R: ProTox-II: a webserver for the prediction of toxicity of chemicals. *Nucleic Acids Research* 2018; 46(1): 257-W263. <https://doi.org/10.1093/nar/gky318>
- Leyrat C, Renner M, Harlos K, Grimes JM and Stuart DI: Structure and self-assembly of the calcium binding matrix protein of human metapneumovirus. *Structure* 2014; 22(1): 136-148. <https://doi.org/10.1016/j.str.2013.10.019>
- Battles MB, Langedijk JP, Furmanova-Hollenstein P, Chaiwatpongsakorn S, Costello HM, Kwanten L, Vranckx L, Vink P, Jaensch S, Jonckers THM, Koul A, Arnoult E, Peeples ME and McLellan JS: Molecular mechanism of respiratory syncytial virus fusion inhibitors. *Nature Chemical Biology* 2017; 13(8): 807-813. <https://doi.org/10.1038/nchembio.2409>
- Selvaraj M, Tripp RA and Samal SK: Molecular characterization of human metapneumovirus M2-1 protein: role in transcriptional regulation and interaction with the phosphoprotein. *Virus Research* 2018; 247: 53-62. <https://doi.org/10.1016/j.virusres.2018.01.012>
- Cox RM, Johnson SK and Williams JV: The human metapneumovirus polymerase complex: Elucidating the structure and function of key viral replication machinery. *PLoS Pathogens* 2019; 15(3): 1007666. <https://doi.org/10.1371/journal.ppat.1007666>
- Buchholz UJ, Yang L, Luongo CL, Skiadopoulos MH, Murphy BR and Collins PL: Structural and functional analysis of the fusion protein of human metapneumovirus. *Journal of Virology* 2005; 79(12): 8122-8130. <https://doi.org/10.1128/JVI.79.12.8122-8130.2005>
- Dallakyan S and Olson AJ: Small-molecule library screening by docking with PyRx. *Methods in Molecular Biology* 2015; 1263: 243-250. https://doi.org/10.1007/978-1-4939-2269-7_19
- Trott O and Olson AJ: AutoDock Vina: Improving the speed and accuracy of docking with a new scoring function, efficient optimization, and multithreading. *Journal of Computational Chemistry* 2010; 31(2): 455-461. <https://doi.org/10.1002/jcc.21334>
- BIOVIA Discovery Studio Visualizer, v21.1.0.20298. (2021). Dassault Systèmes, San Diego: BIOVIA.
- Kousar A, Fathima N, Venkatanagaraju E: *In-silico* Molecular Docking of *Salvadora persica* Metabolites with Myocarditis Causative Coxsackie Virus B3 Capsid Proteins. *Int J Pharm Phytopharmacol Res* 2025; 15(1): 4-12. <https://doi.org/10.51847/NQ7XB0pa4u>
- Lipinski CA, Lombardo F, Dominy BW and Feeney PJ: Experimental and computational approaches to estimate solubility and permeability in drug discovery and development settings. *Advanced Drug Delivery Reviews* 2001; 46(3): 3-26. [https://doi.org/10.1016/S0169-409X\(00\)00129-0](https://doi.org/10.1016/S0169-409X(00)00129-0)

How to cite this article:

Bhargavi VH, Esha A, Javeri MN, Mallikarjun and Venkatanagaraju E: *In-silico* exploration of chyawanprash phytoconstituents binding affinity with key targets of human metapneumovirus. *Int J Pharm Sci & Res* 2026; 17(1): 315-32. doi: 10.13040/IJPSR.0975-8232.17(1).315-32.

All © 2026 are reserved by International Journal of Pharmaceutical Sciences and Research. This Journal licensed under a Creative Commons Attribution-NonCommercial-ShareAlike 3.0 Unported License.

This article can be downloaded to **Android OS** based mobile. Scan QR Code using Code/Bar Scanner from your mobile. (Scanners are available on Google Playstore)